

# DESIGN OF AN L-BAND ACCELERATING STRUCTURE FOR THE ARGONNE WAKEFIELD ACCELERATOR FACILITY WITNESS BEAM LINE ENERGY UPGRADE

J. Shao<sup>1,\*</sup>, J. Power<sup>1</sup>, C. Jing<sup>1,2</sup>, M. Conde<sup>1</sup>, and D. Doran<sup>1</sup>  
<sup>1</sup>Argonne National Laboratory, Lemont, IL 60439, USA  
<sup>2</sup>Euclid Techlabs LLC, Bolingbrook, IL 60440, USA

## Abstract

The Argonne Wakefield Accelerator (AWA) facility has been devoting much effort to the fundamental R&D of two-beam acceleration (TBA) technology with two parallel L-band beam lines. Beginning from the 70 MeV drive beam line, the high frequency (C-band and above) rf power is extracted from the beam by a decelerating structure (a.k.a. power extractor), transferred to an accelerating structure in the witness beam line, and used to accelerate the 15 MeV main beam. These high frequency accelerating structures usually have a small aperture to obtain high gradient and high efficiency, making it difficult for the low energy main beam to pass. To address this issue, one proposal is to increase the main beam energy to above 30 MeV by replacing the current witness linac. A 9-cell  $\pi$ -mode L-band standing-wave accelerating structure has therefore been designed to meet the high shunt impedance and low cost requirements. In addition, the single-feed coupling cell has been optimized with additional symmetrical ports to eliminate field distortion. The detailed design of the new accelerating structure will be presented in this paper.

## INTRODUCTION

TBA is an approach to the structure-based wakefield acceleration which may meet the luminosity, efficiency, and cost requirements of future linear colliders [1]. The AWA facility is a flexible, state-of-art linear collider testbed, aiming to demonstrate  $\sim$ GW rf power generation from the drive beam,  $>300$  MeV/m gradient acceleration of the main beam, and  $>15\%$  wall-to-beam efficiency in TBA and staging. To date, with the unique high-current 70 MeV drive beam line, the AWA facility has successfully achieved 300 MW rf power generation/ 150 MeV/m acceleration TBA and 70 MeV/m staging with X-band metallic structures [2], 55 MW rf power generation/ 28 MeV/m acceleration TBA with K-band dielectric structures, and 105 MW rf power generation with a K-band dielectric power extractor [3]. More TBA activities, such as the full staging with metallic structures [4] and the high efficiency TBA with dielectric disk accelerators [5], are also under investigation at AWA.

Transmitting the main beam through the high frequency high impedance accelerators with small apertures ( $<\phi 10$  mm) is one of the major challenges for TBA experimental research at AWA. Limited by the low main beam energy of 15 MeV, the transmission is usually lower than 40%

and the spectrum information can only be partly revealed. Currently, the main beam is generated in an L-band 1.6-cell photocathode gun (10 MW input power) and accelerated by a low-impedance standing-wave linac (5 MW input power). One solution is to replace the linac with two new designed ones and to raise the input power for the witness beam line. The upgraded beam energy will reach 30 MeV, which will not only improve the transmission of the main beam, but also introduce new opportunities to TBA research at AWA, such as heavy beam-loading study together with the emittance exchange technology [6]. The main requirements of the new linac include high impedance, low cost, and sufficient mode separation. In addition, symmetrical coupling cell is favored to preserve the main beam quality.

## LINACS AT AWA

The current 19-cell witness linac was originally in the drive beam line before the AWA's upgrade in 2014. It applies  $\pi/2$  mode design in which only half of the cells are used to efficiently accelerate the beam, causing low shunt impedance of the whole tube. In the upgrade, six new 7-cell standing-wave linacs, optimized for high-current operation, have been installed in the drive beam line to boost the drive beam energy to 70 MeV [7]. The new drive linac adopts  $\pi$  mode design and its shunt impedance is  $\sim 60\%$  higher than the witness one. The cross sections of the linacs are illustrated in Fig. 1 and the detailed parameter comparison is listed in Table 1.

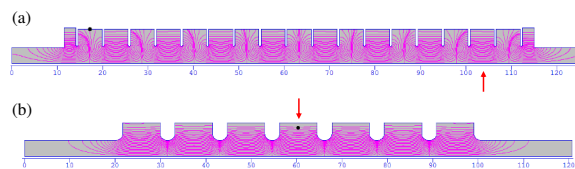


Figure 1: The 2D section view and the electric field distribution of the structures. The red arrow indicates the coupling cell. (a) The witness linac; (b) The drive linac.

## SINGLE CELL DESIGN

The  $\pi$  mode drive linac is a good reference for the design in terms of high shunt impedance, low cost, and high mode separation. The drive linac has been optimized for the high-current bunch train operation with heavy beam loading which is much less prominent in the main beam. Therefore, the shunt impedance can be further improved by ad-

\* jshao@anl.gov

Content from this work may be used under the terms of the CC BY 3.0 licence (© 2018). Any distribution of this work must maintain attribution to the author(s), title of the work, publisher, and DOI.

justing disk thickness and iris diameter. In addition, the rf pulse rise time can be as slow as  $\mu\text{s}$  by adjusting the low level rf system so a smaller mode separation of  $\sim 10$  MHz is adequate for the new witness linac.

Table 1: Comparison Between the Vurrent Witness and Drive Linac

	Witness	Drive
Total cell length (mm)	1036	807
Iris diameter (mm)	101.6	92.0
Disk thickness (mm)	5.02	32.76
Cell coupling (%)	18.85	4.23
Neighbor mode	$4\pi/9$	$2\pi/3$ <sup>1</sup>
Mode separation (MHz)	21.5	14.1
Single cell quality factor	18760	25220
Single cell $r/Q$ (k $\Omega$ /m)	1.16	0.77
Single cell impedance (M $\Omega$ )	1.26	2.25
Whole tube impedance (M $\Omega$ )	9.98	15.70
Input power (MW)	5	10
Energy gain (MeV)	7.06	12.53
Number of bunch per rf pulse	1	1-32
Charge per bunch (nC)	$0.05\text{-}1^2$	10-100

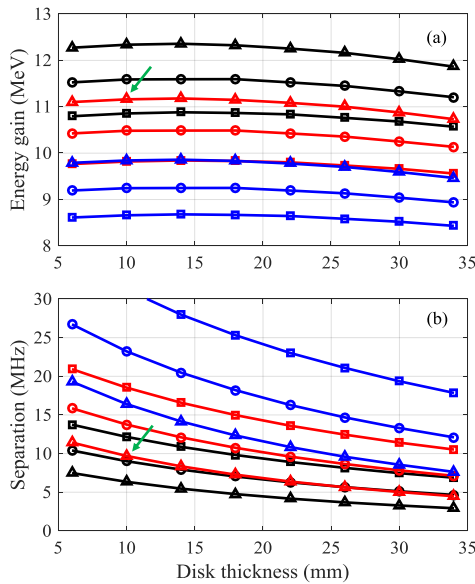


Figure 2: Structure performance with various single cell designs and cell numbers. The blue, the red, and the black line correspond to the 7-cell, 9-cell, and 11-cell structure. The square, the circle, and the triangle curve correspond to the iris diameter of 100 mm, 90 mm, and 80 mm. The green arrow indicates the selected parameters. (a) The unloaded energy gain with 5 MW input power; (b) The mode separation between  $\pi$  mode and the neighbor one.

<sup>1</sup> Due to the symmetry of the field distribution along axis in the drive linac, the  $5\pi/6$  mode would not be excited.

<sup>2</sup> Typical charge for TBA research. A maximum charge of 60 nC per bunch is achievable for other studies.

To improve the energy gain, structures with 7, 9, and 11 cells have been investigated during the optimization, as illustrated in Fig. 2. After comparison, a 9-cell structure with a disk thickness of 10 mm and an iris diameter of 80 mm has been selected for the new design.

## WHOLE TUBE DESIGN

Same as the current drive linac, the new witness linac will be driven from the middle cell by a z-slot single port. To preserve the main beam quality from field distortion, the coupling cell has been improved from the ones in the current witness and drive linacs by adding more ports to obtain symmetrical boundary condition [8], as illustrated in Fig. 3.

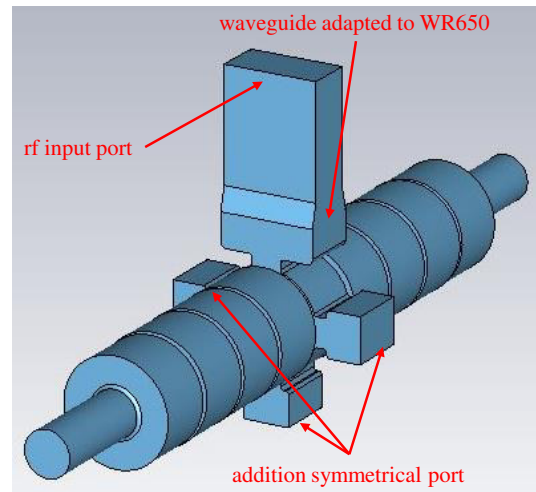


Figure 3: 3D model of the new witness linac in the simulation with CST Microwave Studio.

Dimensions of the additional ports are slight different from the rf input port to fully suppress the dipole and quadrupole field. The magnetic field distribution along the  $\phi$  direction at 10 mm off-axis at the center of the middle cell is illustrated in Fig. 4, from where the dipole and quadrupole field components can be derived by the Fourier transform. Their relative strength to the monopole field is listed in Table 2. The 4-port structure has been selected for the new witness linac design.

Table 2: Relative Strength of the Multipole Field Components

	Dipole field	Quadrupole field
1-port	$1.28 \times 10^{-1}$	$2.73 \times 10^{-2}$
2-port	$7.49 \times 10^{-5}$	$5.59 \times 10^{-2}$
4-port	$4.23 \times 10^{-5}$	$3.99 \times 10^{-4}$

After optimization, the field balance of the middle seven cells is 1; the field of the end cells is  $\sim 7\%$  higher, as illustrated in Fig. 5. Due to the light beam loading, the coupling factor is designed to be 1, as illustrated in Fig. 6.

The detailed parameters of the new designed witness linac are summarized in Table 3. With the same input

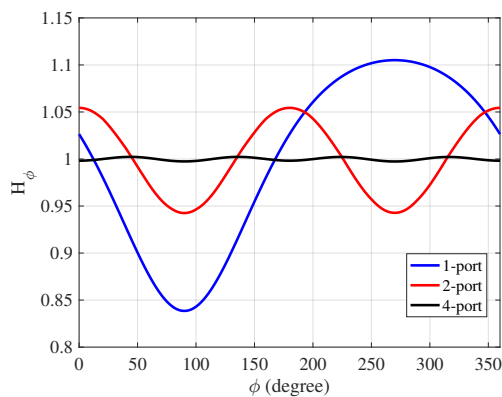


Figure 4: The magnetic field distribution along the  $\phi$  direction at 10 mm off-axis at the center of the middle cell.

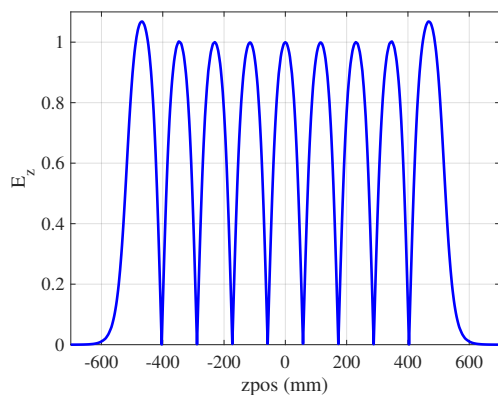


Figure 5: The electric field distribution along the beam axis.

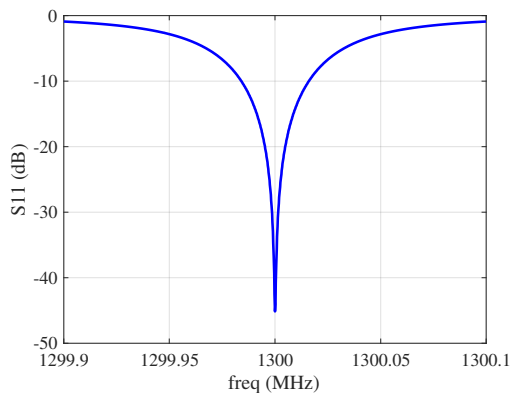


Figure 6: S-parameter of the new witness linac.

power, the energy gain of the new designed witness linac is  $\sim 58\%$  and  $\sim 26\%$  higher than the current witness and drive linac, respectively. When adopting two new designed linacs and raising the input power for the witness beam line to 20 MW from the current level (15 MW), the main beam energy will reach 30 MeV.

## CONCLUSION

A 9-cell high-impedance  $\pi$  mode standing-wave linac has been designed to replace the current witness linac at

Table 3: Parameters of the New Witness Linac

Parameter	value
Total cell length (mm)	1038
Iris diameter (mm)	80
Disk thickness (mm)	10
Cell coupling (%)	4.89
Neighbor mode	$3\pi/4$
Mode separation (MHz)	9.83
Single cell quality factor	27330
Single cell $r/Q$ (k $\Omega$ /m)	0.88
Single cell impedance (M $\Omega$ )	2.78
Whole tube impedance (M $\Omega$ )	24.79
Input power (MW)	5
Energy gain (MeV)	11.13
$E_{max}/E_0$	2.9
Pulse heating (K, with 8 $\mu$ s pulse)	$<2$

AWA to boost the main beam energy. Comparing with the current witness linac, the new designed one has  $\sim 58\%$  higher energy gain while maintaining a low cost. Symmetrical design has been applied in the single-feed coupling cell to significantly suppress the dipole and quadrupole field components. Engineering design of the new witness linac is ongoing at AWA.

## ACKNOWLEDGMENT

The work is funded through the U.S. Department of Energy Office of Science under Contract No. DE-AC02-06CH11357. We would like to thank Dr. Houjun Qian for the valuable discussion on the coupler design.

## REFERENCES

- [1] W. Gai *et al.*, "Short-pulse dielectric two-beam acceleration," *J. Plasma Phys.*, vol. 78, 339-345, 2012.
- [2] J. Shao *et al.*, "Recent two-beam acceleration activities at Argonne Wakefield Accelerator facility," in *Proc. IPAC'2017*, 3305-3307, 2017.
- [3] J. Shao *et al.*, "Recent progress of short pulse dielectric two-beam acceleration," in *Proc. IPAC'2018*, 2018.
- [4] M. Conde *et al.*, "Staging at the Argonne Wakefield Accelerator facility (AWA)," in *Proc. NAPAC'2016*, TUA2IO02, 2016.
- [5] J. Shao *et al.*, "Study of a dielectric disk structure for short pulse two-beam acceleration," in *Proc. IPAC'2018*, 2018.
- [6] G. Ha *et al.*, "Precision control of the electron longitudinal bunch shape using an emittance-exchange beam line," *Phys. Rev. Lett.*, vol. 118, 104801, 2017.
- [7] J. Power *et al.*, "Upgrade of the drive LINAC for the AWA facility dielectric two-beam accelerator," in *Proc. IPAC'2010*, 4310-4312, 2010.
- [8] H. Qian, "Research on the emittance issues of photocathode RF gun," Ph.D. thesis, Tsinghua University, Beijing, China, 2012.